

# Interband electron Raman scattering in a quantum wire in a transverse magnetic field

F.M. Hashimzade<sup>†</sup>, T.G. Ismailov<sup>‡</sup>, B.H. Mehdiyev<sup>†</sup>

<sup>†</sup>*Institute of Physics, Azerbaijan Academy of Sciences, AZ 1143, Baku, Azerbaijan,*

<sup>‡</sup>*Baku State University, AZ 1073/1, Baku, Azerbaijan*

S. T. Pavlov<sup>††</sup>

<sup>†</sup>*Facultad de Fisica de la UAZ, Apartado Postal C-580, 98060 Zacatecas, Zac., Mexico*

<sup>‡</sup>*P. N. Lebedev Physical Institute, Russian Academy of Sciences, 119991 Moscow, Russia*

Electron Raman scattering (ERS) is investigated in a parabolic semiconductor quantum wire in a transverse magnetic field neglecting by phonon-assisted transitions. The ERS cross-section is calculated as a function of a frequency shift and magnetic field. The process involves an interband electronic transition and an intraband transition between quantized subbands. We analyze the differential cross-section for different scattering configurations. We study selection rules for the processes. Some singularities in the Raman spectra are found and interpreted. The scattering spectrum shows density-of-states peaks and interband matrix elements maximums and a strong resonance when scattered frequency equals to the "hybrid" frequency or confinement frequency depending on the light polarization. Numerical results are presented for a GaAs/AlGaAs quantum wire.

PACS numbers: 78.67.Lt; 78.30.Fs

## I. INTRODUCTION

Low-dimensional semiconductor systems, quantum wires in particular, attract considerable attention, because of their novel physical properties and application potential. In recent years a number of innovative techniques have been developed to grow or to fabricate and to study experimentally a variety of quantum wire structures having different geometries and potentials. Many recent experimental and theoretical studies have been performed on quantum wires subjected to a transverse magnetic field [1-7]. Electronic properties of quantum wells in a transverse magnetic field have been investigated in [8-9]. The subband dispersion and magnetoabsorption have been studied for rectangular quantum wires in [10].

A magnetic field perpendicular to the wire axis (a "free electron" direction) can change significantly the electronic states of a semiconductor quantum wire.

Electron Raman scattering seems to be a useful technique providing a direct information on the energy band structure and optical properties of investigated systems [11-13]. In particular, the electronic structure of semiconductor materials and nanostructures can be thoroughly investigated considering different polarizations for the incident and emitted radiation [14]. The differential cross-section, in general case, usually shows singularities related to interband and intraband transitions. This latter result strongly depends on the scattering configurations: the structure of singularities varies when photon polarizations change. This feature of the ERS allows to determine the subband structure of the system by a direct inspection of singularity positions in the spectra. For bulk semiconductors the ERS has been studied in the presence of external magnetic and electric fields [15-17]. In the case of a quantum well preliminary results were reported in [18].

Raman scattering in low-dimensional semiconductor systems has been the subject of many theoretical and experimental investigations [19,20]. Interband ERS processes can be qualitatively described in the following way: absorption of a photon of the incident radiation field creates a virtual electron-hole pair (EHP) in an intermediate crystal state by means of an electron interband transition involving the crystal valence and conduction bands. An electron in the conduction band is subject to a second intraband transition with emission of a secondary radiation photon. Therefore, in the final state we have a real EHP in the crystal and a photon of the secondary radiation. The influence of external fields on such processes for bulk semiconductors is investigated in [16, 17].

In this work we present a systematic study of the interband ERS in a direct band gap semiconducting parabolic quantum wire in a transverse magnetic field. In these systems due to electron confinement and magnetic field the conduction (valence) band is split in a subband system and transitions between them determine ERS processes. Numerical results for the ERS differential cross-section are presented for a GaAs/AlGaAs quantum wire. This article is organized as follows. In Section II the energy spectrum and wave functions for a quantum wire with parabolic confinement potential in a transverse magnetic field are given. In Section III we present the general relations needed for our calculations of the ERS differential cross-section. Section IV is devoted to calculations of ERS differential cross-sections. Finally, Section V is concerned with the discussion of the obtained results.

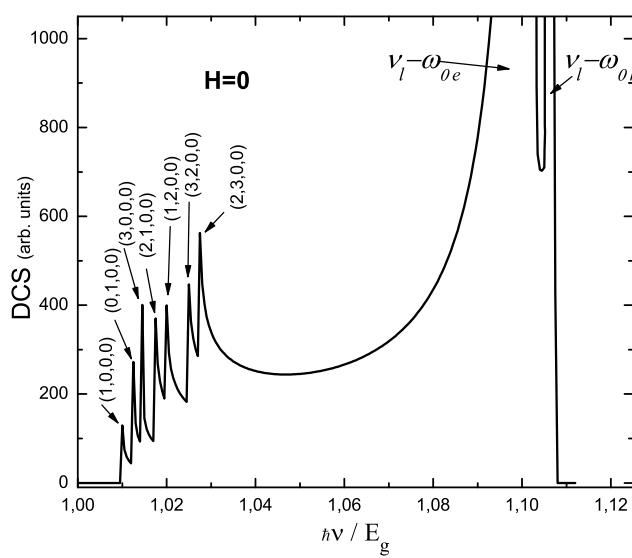


FIG. 1: The Raman spectra of the parabolic quantum wire in the  $X$  scattering configuration for  $H=0$ . The diameter  $d$  of the quantum wire is 2000 Å. The incident radiation frequency  $\hbar\nu_0 = 1.68$  eV. The positions of the singularities are defined by Eqs. (42) and (43). Resonant electron-hole transitions are indicated by  $N_{1h}, N_{1e}, N_{2h}, N_{2e}$ .

## II. WAVE FUNCTIONS AND ENERGY SPECTRUM

We consider a quantum wire aligned along the  $y$  axis with a transverse magnetic field  $\mathbf{H} = \mathbf{H}(0, 0, H)$  applied along the  $z$  axis. The quantum wire is characterized by parabolic confinements in the  $(x, z)$  plane. The effective mass Schrödinger equation for an electron in a conduction band is

$$\left[ \frac{1}{2m_e} \left( \mathbf{p} + \frac{e}{c} \mathbf{A} \right)^2 + \frac{1}{2} m_e \omega_{0e}^2 (x^2 + z^2) \right] \psi_e(x, y, z) = E_e \psi_e(x, y, z), \quad (1)$$

where  $\mathbf{A} = \mathbf{A}(0, xH, 0)$  is the vector potential in the Landau gauge;  $\omega_{0e}$  characterizes the parabolic potential of a quantum wire for electrons in a conduction band;  $m_e, -e$  are the electron effective mass and charge, respectively. We look for the solution in the form

$$\psi_e(x, y, z) = \varphi(x) \eta(z) e^{i p_{y,e} y / \hbar},$$

where  $p_{y,e} = \hbar k_{y,e}$  is the quasi-momentum of an electron.

Shifting the origin of coordinates and separating the variables in the usual way we obtain the eigenfunctions and eigenvalues of the Schrödinger equation (1)

$$\psi_{N_{1e}, N_{2e}, k_{y,e}} = \varphi_{N_{1e}} \left( \frac{x - x_{0e}}{\tilde{L}_e} \right) \eta_{N_{2e}} \left( \frac{z}{L_e} \right) e^{i k_{y,e} y}, \quad (2)$$

$$E_e = (N_{1e} + 1/2) \hbar \tilde{\omega}_e + (N_{2e} + 1/2) \hbar \omega_{0e}$$

$$+ \frac{\hbar^2 k_{y,e}^2}{2m_e} \left( \frac{\omega_{0e}}{\tilde{\omega}_e} \right)^2. \quad (3)$$

The wave functions and energy eigenvalues for electrons in valence band are as follows

$$\psi_{N_{1h}, N_{2h}, k_{y,h}} = \varphi_{N_{1h}} \left( \frac{x - x_{0h}}{\tilde{L}_e} \right) \eta_{N_{2h}} \left( \frac{z}{L_h} \right) e^{i k_{y,h} y}, \quad (4)$$

$$E_h = -E_g - (N_{1h} + 1/2) \hbar \tilde{\omega}_h + (N_{2h} + 1/2) \hbar \omega_{0h} - \frac{\hbar^2 k_{y,h}^2}{2m_h} \left( \frac{\omega_{0h}}{\tilde{\omega}_h} \right)^2, \quad (5)$$

where  $E_g$  is the energy gap between the valence and conduction bands in absence of an external magnetic field,  $\omega_{0h}$  is the oscillator frequency of the parabolic potential for electrons in the valence band. In Eqs. (2) - (5)

$$\tilde{\omega}_{e,h} = \sqrt{\omega_{0e(h)}^2 + \omega_{e(h)}^2} \quad (6)$$

is the "hybrid" frequency. The subscripts  $e$  and  $h$  denote conduction and valence band, respectively.

$$\omega_{e(h)} = \frac{eH}{m_{e(h)} c} \quad (7)$$

is the cyclotron frequency,  $m_{e(h)}$  is the effective mass,

$$x_{0e(h)} = \frac{\hbar \omega_{e(h)}}{m_{e(h)} \tilde{\omega}_{e(h)}^2} \cdot k_{y,e(h)} \quad (8)$$

is the oscillator centre.

The full energy spectrum in (2) - (5) is governed by quantum numbers  $N_{1e(h)}, N_{2e(h)}$  and  $k_{y,e(h)}$ .

$$\varphi_{N_{1e(h)}} \left( \frac{x - x_{0e(h)}}{\tilde{L}_{e(h)}} \right) = \left( \frac{1}{\pi \tilde{L}_{e(h)}^2} \right)^{1/4} \frac{1}{\sqrt{2^{N_{1e(h)}} N_{1e(h)}}!} \times \exp \left( -\frac{(x - x_{0e(h)})^2}{2 \tilde{L}_e^2} \right) H_{N_{1e(h)}} \left( \frac{x - x_{0e(h)}}{\tilde{L}_{e(h)}} \right), \quad (9)$$

$$\eta_{N_{2e(h)}} \left( \frac{z}{L_{e(h)}} \right) = \left( \frac{1}{\pi L_{e(h)}^2} \right)^{1/4} \frac{1}{\sqrt{2^{N_{2e(h)}} N_{2e(h)}}!} \times \exp \left( -\frac{z^2}{2 L_{e(h)}^2} \right) H_{N_{2e(h)}} \left( \frac{z}{L_{e(h)}} \right), \quad (10)$$

where parameters

$$\tilde{L}_{e(h)} = \sqrt{\frac{\hbar}{m_{e(h)} \tilde{\omega}_{e(h)}}}; \quad L_{e(h)} = \sqrt{\frac{\hbar}{m_{e(h)} \omega_{0e(h)}}} \quad (11)$$

are the units of length;  $H_n(\xi)$  is the Hermitian polynomial.

### III. PRELIMINARY RELATIONS

The general expression for the ERS differential cross-section is given by [16,18]

$$\frac{d^2\sigma}{d\Omega d\nu_s} = \frac{V^2 \nu_s^2 n(\nu_s)}{8\pi^3 c^4 n(\nu_l)} W(\nu_s, \mathbf{e}_s) \quad (12)$$

where  $c$  is the light velocity in vacuum,  $n(\nu)$  is refraction index as a function of the radiation frequency,  $\mathbf{e}_s$  the (unit) polarization vector for the secondary radiation field,  $V$  is the normalization volume,  $\nu_s$  is the secondary radiation frequency,  $\nu_l$  is the frequency of the incident radiation.  $W(\nu_s, \mathbf{e}_s)$  is the transition rate calculated according to

$$W(\nu_s, \mathbf{e}_s) = \frac{2\pi}{\hbar} \sum_f |M_e + M_h|^2 \delta(E_f - E_i), \quad (13)$$

where

$$M_j = \sum_a \frac{\langle f | \hat{H}_{js} | a \rangle \langle a | \hat{H}_l | i \rangle}{E_i - E_a} + \sum_b \frac{\langle f | \hat{H}_l | b \rangle \langle b | \hat{H}_{js} | i \rangle}{E_i - E_b}. \quad (14)$$

In (14)  $j = e, h$  are for the cases of electrons or holes, respectively,  $|i\rangle$  and  $|f\rangle$  denote initial and final states of the system with their corresponding energies  $E_i$  and  $E_f$ .  $|a\rangle$  and  $|b\rangle$  are intermediate states with energies  $E_a$  and  $E_b$ .

The operator  $\hat{H}_l$  is of the form

$$\hat{H}_l = \frac{|e|}{m_0} \sqrt{\frac{2\pi\hbar}{V\nu_l}} \mathbf{e}_l \cdot \hat{\mathbf{p}}, \quad \hat{\mathbf{p}} = -i\hbar\nabla, \quad (15)$$

where  $m_0$  is the free electron mass. This operator describes the interaction with the incident radiation field in the dipol approximation. The interaction with the secondary -radiation field is described by the operator

$$\hat{H}_{js} = \frac{|e|}{m_j} \sqrt{\frac{2\pi\hbar}{V\nu_s}} \mathbf{e}_s \cdot \hat{\mathbf{p}}, \quad j=e, h. \quad (16)$$

This Hamiltonian describes the photon emission by the electron (hole) after transitions between conduction (valence) subbands of the system. In (14) the intermediate states  $|a\rangle$  represent an EHP in a virtual state (after absorption of the incident photon), while the states  $|b\rangle$  are related to the “interference diagrams” [16,18]. This latter term involves a negligible contribution whenever the energy gap  $E_g$  is large enough (for instance, this is the case for  $GaAs$ ) and will not be considered in the present work.

We established that the processes of ERS given in following are possible:

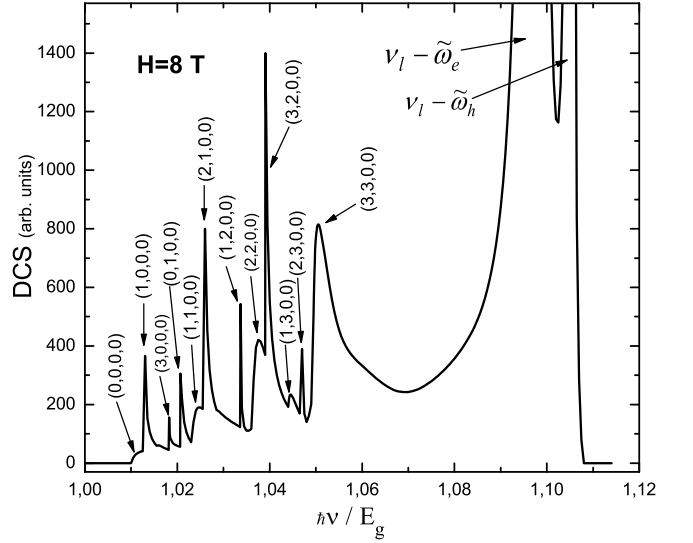


FIG. 2: Same that in Fig.1 for  $H = 8T$ .

**a) The interband ERS process with the intermediate state in the conduction band.** First, an incident light quantum is being absorbed creating an electron -hole pair between the state  $(N_{1h}, N_{2h})$  in the valence band and the state  $(N'_{1e}, N'_{2e})$  in the conduction band. Second, a scattered photon is emitted due to an electronic transition from the state  $(N'_{1e}, N'_{2e})$  to the state  $(N_{1e}, N_{2e})$  in the conduction band. The Raman shift  $\hbar\nu = \hbar(\nu_l - \nu_s)$  is equal to the excitation energy of the electron-hole pair created in the scattering process.

**b) The interband ERS process with the intermediate state in the valence band.** Two electrons take part in the process. After the absorption of incident photon the first electron from the state  $(N'_{1h}, N'_{2h})$  in valence band is lifted to the state  $(N_{1e}, N_{2e})$ . The second electron from the state  $(N_{1h}, N_{2h})$  falls to the vacant state in the  $(N'_{1h}, N'_{2h})$  subband. The real transition corresponds to a transition from the state  $(N_{1h}, N_{2h})$  to the state  $(N_{1e}, N_{2e})$ .

In the initial state  $|i\rangle$  we have an incident radiation photon with frequency  $\nu_l$ , while the conduction band is empty and the valence band completely occupied by electrons. We neglect by all the transitions assisted by phonons.

The initial state energy is

$$E_i = \hbar\nu_l. \quad (17)$$

The final state of the process consists of an EHP in a real state and a scattered light with energy  $\hbar\nu_s$ . Thus,

$$E_f = \hbar\nu_s + E_{N_{1h}} + E_{N_{2h}} + E_{N_{1e}} + E_{N_{2e}} + E_g$$

$$+\frac{\hbar^2 k_{ye}^2}{2m_e} \left( \frac{\omega_{0e}}{\tilde{\omega}_e} \right)^2 + \frac{\hbar^2 k_{yh}^2}{2m_h} \left( \frac{\omega_{0h}}{\tilde{\omega}_h} \right)^2, \quad (18)$$

where

$$\begin{aligned} E_{N_{1e(h)}} &= (N_{1e(h)} + 1/2)\hbar\tilde{\omega}_{e(h)}, \\ E_{N_{2e(h)}} &= (N_{2e(h)} + 1/2)\hbar\omega_{0e(h)}. \end{aligned} \quad (19)$$

For the electron intermediate states  $|a\rangle$  the energies  $E_a$  are easily obtained from the above discussion.

$$\begin{aligned} E_i - E_a &= -E_g - E_{N_{1h}} - E_{N_{2h}} - E_{N'_{1e}} - E_{N'_{2e}} \\ &\quad - \frac{\hbar^2 k_{ye}^2}{2m_e} \left( \frac{\omega_{0e}}{\tilde{\omega}_e} \right)^2 - \frac{\hbar^2 k_{yh}^2}{2m_h} \left( \frac{\omega_{0h}}{\tilde{\omega}_h} \right)^2 + \hbar\nu_l. \end{aligned} \quad (20)$$

Similar expressions can be written for the hole intermediate state energies.

#### IV. CALCULATION OF THE RAMAN SCATTERING CROSS SECTION

The matrix elements of the intraband transitions may be written as

$$\begin{aligned} &\frac{|e|}{m_e} \sqrt{\frac{2\pi\hbar}{V\nu_s}} \langle N_{1e}, N_{2e}, k_{ye} | \mathbf{e}_s \mathbf{p} | N'_{1e} N'_{2e}, k'_{ye} \rangle = \\ &= \frac{|e|}{m_e} \sqrt{\frac{2\pi\hbar}{V\nu_s}} [\langle N_{1e}, N_{2e}, k_{ye} | e_{sx} p_x | N'_{1e} N'_{2e}, k'_{ye} \rangle + \\ &+ \langle N_{1e}, N_{2e}, k_{ye} | e_{sy} p_y | N'_{1e} N'_{2e}, k'_{ye} \rangle + \\ &+ \langle N_{1e}, N_{2e}, k_{ye} | e_{sz} p_z | N'_{1e} N'_{2e}, k'_{ye} \rangle], \end{aligned} \quad (21)$$

where

$$\begin{aligned} \langle N_{1e}, N_{2e}, k_{ye} | e_{sx} p_x | N'_{1e} N'_{2e}, k'_{ye} \rangle &= -\frac{i\hbar}{\tilde{L}_e} e_{sx} \delta_{N'_{2e}, N_{2e}} \\ &\times \left[ \sqrt{\frac{N_{1e}}{2}} \delta_{N'_{1e}, N_{1e}-1} - \sqrt{\frac{N_{1e}+1}{2}} \delta_{N'_{1e}, N_{1e}+1} \right] \\ &\times \delta_{k_{ye}, k'_{ye}}, \end{aligned} \quad (22)$$

$$\begin{aligned} \langle N_{1e}, N_{2e}, k_{ye} | e_{sy} p_y | N'_{1e} N'_{2e}, k'_{ye} \rangle &= \\ &= \hbar k'_{ye} e_{sy} \delta_{N'_{2e}, N_{2e}} \delta_{N'_{2e}, N_{2e}} \delta_{k_{ye}, k'_{ye}}, \end{aligned} \quad (23)$$

$$\begin{aligned} \langle N_{1e}, N_{2e}, k_{ye} | e_{sz} p_z | N'_{1e} N'_{2e}, k'_{ye} \rangle &= -\frac{i\hbar}{\tilde{L}_e} e_{sz} \delta_{N'_{1e}, N_{1e}} \\ &\times \left[ \sqrt{\frac{N_{2e}}{2}} \delta_{N'_{2e}, N_{2e}-1} - \sqrt{\frac{N_{2e}+1}{2}} \delta_{N'_{2e}, N_{2e}+1} \right] \\ &\times \delta_{k_{ye}, k'_{ye}}. \end{aligned} \quad (24)$$

A similar expression can be written for the interband ERS process with the intermediate state in the valence

band

$$\begin{aligned} &\frac{|e|}{m_h} \sqrt{\frac{2\pi\hbar}{V\nu_s}} \langle N'_{1h}, N'_{2h}, k'_{yh} | \mathbf{e}_s \mathbf{p} | N_{1h}, N_{2h}, k_{yh} \rangle = \\ &= \frac{|e|}{m_h} \sqrt{\frac{2\pi\hbar}{V\nu_s}} [\langle N'_{1h}, N'_{2h}, k'_{yh} | e_{sx} p_x | N_{1h}, N_{2h}, k_{yh} \rangle \\ &+ \langle N'_{1h}, N'_{2h}, k'_{yh} | e_{sy} p_y | N_{1h}, N_{2h}, k_{yh} \rangle \\ &+ \langle N'_{1h}, N'_{2h}, k'_{yh} | e_{sz} p_z | N_{1h}, N_{2h}, k_{yh} \rangle], \end{aligned} \quad (25)$$

where

$$\begin{aligned} &\langle N'_{1h}, N'_{2h}, k'_{yh} | e_{sx} p_x | N_{1h}, N_{2h}, k_{yh} \rangle = \\ &= -\frac{i\hbar}{\tilde{L}_h} e_{sx} \delta_{N_{2h}, N'_{2h}} \\ &\times \left[ \sqrt{\frac{N_{1h}+1}{2}} \delta_{N_{1h}, N'_{1h}-1} - \sqrt{\frac{N_{1h}}{2}} \delta_{N_{1h}, N'_{1h}+1} \right] \\ &\times \delta_{k_{yh}, k'_{yh}}, \end{aligned} \quad (26)$$

$$\begin{aligned} \langle N'_{1h}, N'_{2h}, k'_{yh} | e_{sy} p_y | N_{1h}, N_{2h}, k_{yh} \rangle &= \\ &= \hbar k_{yh} e_{sy} \delta_{N_{2h}, N'_{2h}} \delta_{N_{1h}, N'_{1h}} \delta_{k_{yh}, k'_{yh}}, \end{aligned} \quad (27)$$

$$\begin{aligned} &\langle N'_{1h}, N'_{2h}, k'_{yh} | e_{sz} p_z | N_{1h}, N_{2h}, k_{yh} \rangle = \\ &\times -\frac{i\hbar}{\tilde{L}_h} e_{sz} \delta_{N_{1h}, N'_{1h}} \\ &\times \left[ \sqrt{\frac{N_{2h}+1}{2}} \delta_{N_{2h}, N'_{2h}-1} - \sqrt{\frac{N_{2h}}{2}} \delta_{N_{2h}, N'_{2h}+1} \right] \\ &\times \delta_{k_{yh}, k'_{yh}}. \end{aligned} \quad (28)$$

If we consider allowed electron transitions between conduction and valence bands, the interband matrix element in the envelope function approximation, may be written as

$$\begin{aligned} \langle a | \hat{H}_l | i \rangle &= \frac{|e|}{m_0} \sqrt{\frac{2\pi\hbar}{V\nu_l}} (\mathbf{p}_{cv} \mathbf{e}_l) \\ &\times \begin{cases} I_{N_{1h}, N'_{1e}}(k_y) J_{N_{2h}, N'_{2e}} \delta_{k_{yh}, k'_{ye}}, & j = e; \\ I_{N'_{1h}, N_{1e}}(k_y) J_{N'_{2h}, N_{2e}} \delta_{k'_{yh}, k_{ye}}, & j = h, \end{cases} \end{aligned} \quad (29)$$

where  $\mathbf{p}_{cv}$  is the momentum matrix element between the valence and conduction bands (evaluated at  $\mathbf{k} = 0$ ).

We find that the matrix elements (22)-(29) vanish unless the following selection rule is satisfied

$$k_{ye} = k_{yh} = k'_{ye} = k'_{yh} = k_y. \quad (30)$$

The EHP does not change its total momentum during absorption or emission of a photon (a photon momentum is neglected). It may be obtained that

$$I_{N_{1h}, N'_{1e}}(k_y) = \left( \frac{1}{\pi} \right)^{1/2} \left( \frac{1}{\tilde{L}_h \tilde{L}_e} \right)^{1/2}$$

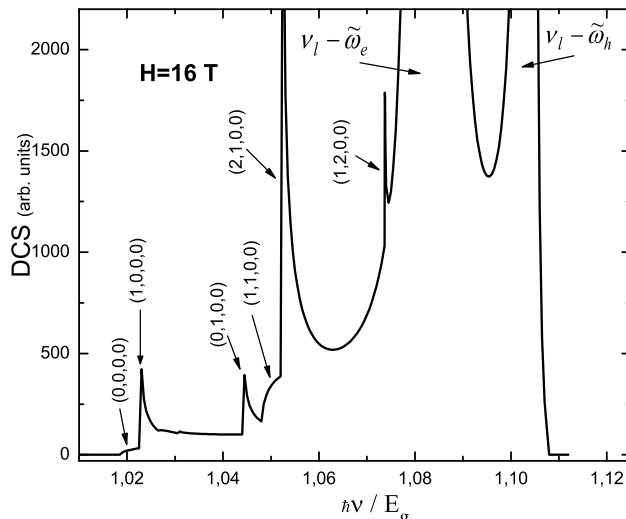


FIG. 3: Same that in Fig.1 for  $H = 16T$ .

$$\begin{aligned}
&\times \frac{N_{1h}!N'_{1e}!}{\sqrt{2^{N_{1h}+N'_{1e}}N_{1h}!N'_{1e}!}} \\
&\times \sum_{k=0}^{[N_{1h}/2]} \sum_{j=0}^{[N'_{1e}/2]} \frac{(-1)^{k+j} 2^{N_{1h}+N'_{1e}-2k-2j}}{k!j!(N_{1h}-2k)!(N'_{1e}-2j)!} \\
&\times \left(\frac{1}{\tilde{L}_e}\right)^{N'_{1e}-2j} \left(\frac{1}{\tilde{L}_h}\right)^{N_{1h}-2k} \sum_{\mu=0}^{N_{1h}-2k} \frac{(N_{1h}-2k)!}{\mu!(N_{1h}-2k-\mu)!} \\
&\times (x_{0e} - x_{0h})^{N_{1h}-2k-\mu} \sum_{\nu=0}^{N'_{1e}-2j+\mu} \frac{(N'_{1e}-2j+\mu)!}{\nu!(N'_{1e}-2j+\mu-\nu)!} \\
&\times [(-1)^\nu + 1] \exp\left(\frac{-(x_{0e} - x_{0h})^2}{2(\tilde{L}_e^2 + \tilde{L}_h^2)}\right) \\
&\times \frac{1}{2} \left(\frac{\tilde{L}_e^2 + \tilde{L}_h^2}{2\tilde{L}_e^2\tilde{L}_h^2}\right)^{-(\nu+1)/2} \\
&\times \Gamma\left(\frac{\nu+1}{2}\right) \left(-\frac{\tilde{L}_e^2(x_{0e} - x_{0h})}{\tilde{L}_e^2 + \tilde{L}_h^2}\right)^{N'_{1e}-2j+\mu-\nu} \quad (31)
\end{aligned}$$

and

$$\begin{aligned}
J_{N_{2h},N'_{2e}} &= \left(\frac{1}{\pi}\right)^{1/2} \left(\frac{1}{L_h L_e}\right)^{1/2} \sqrt{\frac{N_{2h}!N'_{2e}!}{2^{N_{2h}+N'_{2e}}}} \\
&\times \sum_{\alpha=0}^{[N'_{2e}/2]} \sum_{\beta=0}^{[N_{2h}/2]} \frac{(-1)^{\alpha+\beta} 2^{N'_{2e}-2\alpha+N_{2h}-2\beta}}{\alpha!\beta!(N'_{2e}-2\alpha)!(N_{2h}-2\beta)!} \\
&\times \left(\frac{1}{L_e}\right)^{N'_{2e}-2\alpha} \left(\frac{1}{L_h}\right)^{N_{2h}-2\beta} [(-1)^{N'_{2e}+N_{2h}-2\alpha-2\beta} + 1]
\end{aligned}$$

$$\times \frac{\Gamma\left(\frac{N'_{2e}+N_{2h}-2\alpha-2\beta+1}{2}\right)}{2\left(\frac{\sqrt{L_e^2+L_h^2}}{\sqrt{2}L_h L_e}\right)^{N'_{2e}+N_{2h}-2\alpha-2\beta+1}}. \quad (32)$$

An expression analogous to Eqs. (31) and (32) holds for  $I_{N'_{1h},N'_{1e}}(k_y)$  and  $J_{N'_{2h},N'_{2e}}$  after making the replacements  $N_{1h} \rightarrow N'_{1h}$  and  $N_{2h} \rightarrow N'_{2h}$ .

Performing the summation over  $k_y$  in (13) we obtain the ERS differential cross section:

$$\begin{aligned}
\frac{d^2\sigma}{d\Omega d\nu_s} &= \left(\frac{d^2\sigma}{d\Omega d\nu_s}\right)_{e_{sx}} + \left(\frac{d^2\sigma}{d\Omega d\nu_s}\right)_{e_{sy}} \\
&+ \left(\frac{d^2\sigma}{d\Omega d\nu_s}\right)_{e_{sz}}, \quad (33)
\end{aligned}$$

where

$$\begin{aligned}
&\left(\frac{d^2\sigma}{d\Omega d\nu_s}\right)_{e_{sx}} = \frac{\sigma_0}{\tilde{L}_e^2} \frac{\nu_l - \nu}{\nu_l} \\
&\times \sum_{N_{1e},N_{2e},N_{1h},N_{2h}} \left[ \sum_{N'_{1e},N'_{2e},N'_{1h},N'_{2h}} \right. \\
&\times \left\{ \frac{\beta}{A(\nu)} \delta_{N_{2e},N'_{2e}} \right. \\
&\times \left( \sqrt{N_{1e}/2} \cdot \delta_{N'_{1e},N_{1e}-1} - \sqrt{(N_{1e}+1)/2} \cdot \delta_{N'_{1e},N_{1e}+1} \right) \\
&\times I_{N_{1h},N'_{1e}}(k_y(\nu)) J_{N_{2h},N'_{2e}} \\
&+ \frac{\gamma(H)}{B(\nu)} \delta_{N_{2h},N'_{2h}} I_{N'_{1h},N_{1e}}(k_y(\nu)) J_{N'_{2h},N_{2e}} \\
&\times \left. \left( \sqrt{\frac{N_{1h}+1}{2}} \delta_{N_{1h},N'_{1h}-1} - \sqrt{\frac{N_{1h}}{2}} \delta_{N_{1h},N'_{1h}+1} \right) \right]^2 \\
&\times \left( \frac{E_g}{\hbar\nu - E_{N_{1e}} - E_{N_{1h}} - E_{N_{2e}} - E_{N_{2h}} - E_g} \right)^{1/2} \\
&\times |\mathbf{e}_s \cdot \mathbf{X}|^2, \quad (34)
\end{aligned}$$

and

$$\begin{aligned}
&\left(\frac{d^2\sigma}{d\Omega d\nu_s}\right)_{e_{sy}} = \frac{\sigma_0}{L_e^2} \frac{\nu_l - \nu}{\nu_l} \\
&\times \sum_{N_{1e},N_{2e},N_{1h},N_{2h}} \left[ \sum_{N'_{1e},N'_{2e},N'_{1h},N'_{2h}} \right. \\
&\times \left\{ \frac{\beta}{A(\nu)} I_{N_{1h},N'_{1e}}(k_y(\nu)) J_{N_{2h},N'_{2e}} \delta_{N_{2e},N'_{2e}} \delta_{N_{1e},N'_{1e}} \right. \\
&+ \frac{1}{B(\nu)} I_{N'_{1h},N_{1e}}(k_y(\nu)) J_{N'_{2h},N_{2e}} \delta_{N_{2h},N'_{2h}} \delta_{N_{1h},N'_{1h}} \left. \right\}^2 \\
&\times \left( \frac{E_g}{\hbar\nu - E_{N_{1e}} - E_{N_{1h}} - E_{N_{2e}} - E_{N_{2h}} - E_g} \right)^{1/2} \\
&\times (k_y(\nu)L_e)^2 |\mathbf{e}_s \cdot \mathbf{Y}|^2, \quad (35)
\end{aligned}$$

$$\left(\frac{d^2\sigma}{d\Omega d\nu_s}\right)_{e_{sz}} = \frac{\sigma_0}{L_e} \frac{\nu_l - \nu}{\nu_l}$$

$$\begin{aligned}
& \times \sum_{N_{1e}, N_{2e}, N_{1h}, N_{2h}} \left[ \sum_{N'_{1e}, N'_{2e}, N'_{1h}, N'_{2h}} \left\{ \frac{\beta}{A(\nu)} \delta_{N_{2e}, N'_{2e}} \right. \right. \\
& \times \left. \left. \left( \sqrt{N_{2e}/2} \cdot \delta_{N'_{2e}, N_{2e}-1} - \sqrt{(N_{2e}+1)/2} \cdot \delta_{N'_{2e}, N_{2e}+1} \right) \right. \right. \\
& \times I_{N_{1h}, N'_{1e}}(k_y(\nu)) J_{N_{2h}, N'_{2e}} \\
& + \frac{\gamma}{B(\nu)} \delta_{N_{1h}, N'_{1h}} I_{N'_{1h}, N_{1e}}(k_y(\nu)) J_{N'_{2h}, N_{2e}} \\
& \times \left( \sqrt{\frac{N_{2h}+1}{2}} \delta_{N_{2h}, N'_{2h}-1} - \sqrt{\frac{N_{2h}}{2}} \delta_{N_{2h}, N'_{2h}+1} \right)^2 \\
& \times \left( \frac{E_g}{\hbar\nu - E_{N_{1e}} - E_{N_{1h}} - E_{N_{2e}} - E_{N_{2h}} - E_g} \right)^{1/2} \\
& \times |\mathbf{e}_s \cdot \mathbf{Z}|^2, \quad (36)
\end{aligned}$$

where

$$\begin{aligned}
\sigma_0 = & \frac{e^4 L_y |\mathbf{p}_{cv} \mathbf{e}_l|^2 \hbar^2 n(\nu_s)}{\sqrt{2} \pi m_0^2 m_h^2 E_g^{5/2} n(\nu_l) c^4} \\
& \times \frac{1}{\sqrt{\frac{1}{m_e} \left( \frac{\omega_{0e}}{\omega_e} \right)^2 + \frac{1}{m_h} \left( \frac{\omega_{0h}}{\omega_h} \right)^2}}; \quad (37)
\end{aligned}$$

$$A(\nu) = \frac{\hbar}{E_g} [\nu - \nu_l + (N_{2e} - N'_{2e}) \omega_{0e} + (N_{1e} - N'_{1e}) \tilde{\omega}_e], \quad (38)$$

$$B(\nu) = \frac{\hbar}{E_g} [(N'_{2h} - N_{2h}) \omega_{0h} + (N'_{1h} - N_{1h}) \tilde{\omega}_h - \nu + \nu_l], \quad (39)$$

$$\beta = \frac{m_h}{m_e}, \quad \gamma(H) = \frac{\tilde{L}_e}{\tilde{L}_h}, \quad \gamma = \frac{L_e}{L_h} \quad (40)$$

and  $k_y(\nu)$  is the root of the delta function argument

$$|k_y(\nu)| = \frac{\sqrt{2}}{\hbar} \sqrt{\frac{\hbar\nu - E_g - E_{N_{1e}} - E_{N_{1h}} - E_{N_{2e}} - E_{N_{2h}}}{\frac{1}{m_e} \left( \frac{\omega_{0e}}{\omega_e} \right)^2 + \frac{1}{m_h} \left( \frac{\omega_{0h}}{\omega_h} \right)^2}}. \quad (41)$$

The vectors  $\mathbf{X}$ ,  $\mathbf{Y}$  and  $\mathbf{Z}$  are unit vectors along the corresponding Cartesian axes.

Let us make some remarks concerning the above equations. As indicated above, when  $\hbar\nu > E_g$  the Raman process involves the combination of intraband and interband transitions. From Eq. (32) it follows that  $J_{N_{2h}, N'_{2e}} (J_{N'_{2h}, N_{2e}})$  vanishes unless  $N_{2h} + N'_{2e} = 2n$  ( $N'_{2h} + N_{2e} = 2n$ ) where  $n$  is an integer. So, transition can only take place between  $N_{2h}$  and  $N'_{2e}$  ( $N'_{2h}$  and  $N_{2e}$ ) subbands with the same parity ( $2m \rightarrow 2n$ ; and  $2m+1 \rightarrow 2n+1$ ;  $m$  and  $n$  are integers). But for Eq. (31) quantum numbers  $N_{1h}$  and  $N'_{1e}$  ( $N'_{1h}$  and  $N_{1e}$ ) can change arbitrarily.

Hence, the following selection rules are obtained for interband transitions:

$$|N_{1h} - N'_{1e}| = 0, 1, 2, \dots; \quad |N_{2h} - N'_{2e}| = 0, 2, 4 \dots;$$

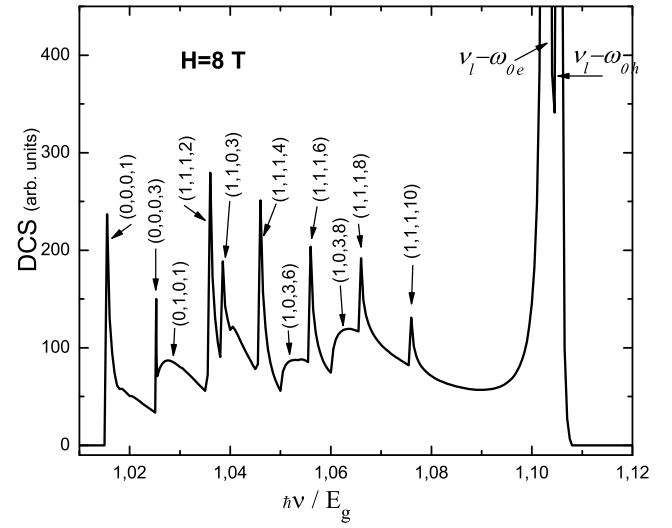


FIG. 4: The Raman spectra for the  $Z$  scattering configuration for the magnetic fields  $H = 8T$ . Other parameters coincide with those of Figs. 1-3.

$$|N'_{1h} - N_{1e}| = 0, 1, 2, \dots; \quad |N'_{2h} - N_{2e}| = 0, 2, 4 \dots;$$

1. When  $H = 0$ ,  $x_{0e} = x_{0h} = 0$ ,  $\tilde{L}_e = L_e$  and  $\tilde{L}_h = L_h$  that is the oscillator center of the conduction and valence band electrons coincident. Then, making the replacement  $N_{2h} \rightarrow N_{1h}$ ,  $N'_{2e} \rightarrow N'_{1e}$  ( $N'_{2h} \rightarrow N'_{1h}$ ,  $N_{2e} \rightarrow N_{1e}$ ), we see that Eq.(31) turns into Eq.(32). Thus, for  $H = 0$  we have the selection rules

$$|N_{1h} - N'_{1e}| = 0, 2, 4 \dots; |N_{2h} - N'_{2e}| = 0, 2, 4 \dots;$$

$$|N'_{1h} - N_{1e}| = 0, 2, 4 \dots; |N'_{2h} - N_{2e}| = 0, 2, 4 \dots.$$

2. The case  $\omega_{e(h)} \gg \omega_{0e(h)}$ . This condition corresponds to the strong magnetic fields, and we have

$$\tilde{\omega}_{e(h)} = \omega_{e(h)} \sqrt{1 + \left( \frac{\omega_{0e(h)}}{\omega_{e(h)}} \right)^2} \approx \omega_{e(h)}$$

and

$$x_{0e} \approx x_{0h}, \quad \tilde{L}_e \approx \tilde{L}_h = \sqrt{\frac{c\hbar}{eH}} = l_H,$$

where  $l_H$  is the magnetic length. For this case Eq. (31) differs from zero when  $N_{1h} = N'_{1e}$  ( $N'_{1h} = N_{1e}$ ). In this way, the selection rule  $|N_{2h} - N'_{2e}| = 2n+1$  ( $|N'_{2h} - N_{2e}| = 2n+1$ ) takes place in intermediate magnetic fields.

As can be seen from Eqs. (34) and (36) the differential cross section is directly proportional to the density-of-states of carriers in the valence and conduction bands and

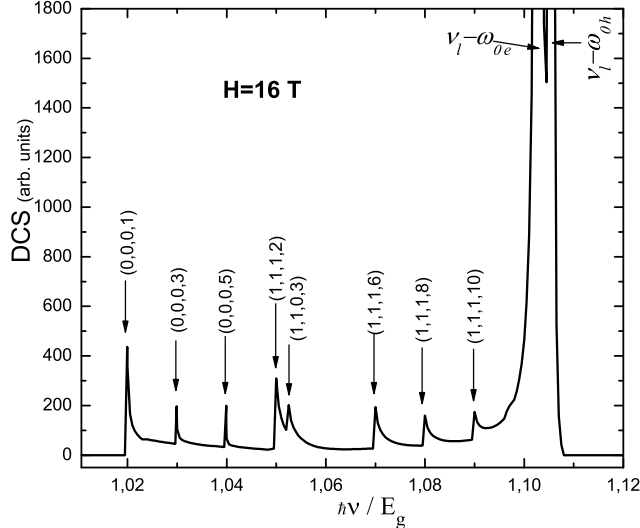


FIG. 5: The Raman spectra for the  $Z$  scattering configuration for the magnetic fields  $H = 16T$ . Other parameters coincide with those of Figs. 1-3.

to the interband matrix elements. In this case the scattering spectrum shows density-of-states peaks and interband matrix elements maximums. The positions of these structures are given as follows:

$$\hbar\nu = E_{N_{1h}} + E_{N_{2h}} + E_{N_{1e}} + E_{N_{2e}} + E_g. \quad (42)$$

Here, the following selection rules must be fulfilled:  $N'_{1e} = N_{1e} \pm 1$ ,  $N'_{2e} = N_{2e}$  ( $N'_{1h} = N_{1h} \pm 1$ ,  $N'_{2h} = N_{2h}$ ) for  $X$  scattering configuration and  $N'_{2e} = N_{2e} \pm 1$ ,  $N'_{1e} = N_{1e}$  ( $N'_{2h} = N_{2h} \pm 1$ ,  $N'_{1h} = N_{1h}$ ) for  $Z$  scattering configuration. In this case when  $|N_{1h} - N'_{1e}| = 2n + 1$  ( $|N'_{1h} - N_{1e}| = 2n + 1$ ) the spectrum shows maximums and when  $|N_{1h} - N'_{1e}| = 2n$  ( $|N'_{1h} - N_{1e}| = 2n$ ) the ERS spectrum shows singular peaks. The peaks and maximums related to these structures correspond to interband EHP transitions and their positions depend on the magnetic field.

Other singularities of equations (34) and (36) occur whenever  $A(\nu) = 0$  and  $B(\nu) = 0$ . In the  $X$  scattering configuration this singularities are

$$\nu = \nu_l - \tilde{\omega}_e, \quad \nu = \nu_l - \tilde{\omega}_h. \quad (43)$$

Here the following selection rules are fulfilled:  $N'_{1e} = N_{1e} + 1$ ,  $N'_{2e} = N_{2e}$  and  $N'_{1h} = N_{1h} - 1$ ,  $N'_{2h} = N_{2h}$ .

For the  $Z$  scattering configuration the Raman singularity is

$$\nu = \nu_l - \omega_{0e}, \quad \nu = \nu_l - \omega_{0h}. \quad (44)$$

In this case the selection rules are:  $N'_{1e} = N_{1e}$ ,  $N'_{2e} = N_{2e} + 1$  and  $N'_{1h} = N_{1h}$ ,  $N'_{2h} = N_{2h} - 1$ .

As can be seen from equations (43) and (44) these frequencies correspond to electron transitions connecting the subband edges for a process involving the conduction and valence bands (i.e., intraband transitions). We can also notice that the  $Y$  scattering configuration is free from Raman singularity and relates to selection rules:  $N'_{1e} = N_{1e}$ ,  $N'_{2e} = N_{2e}$  and  $N'_{1h} = N_{1h}$ ,  $N'_{2h} = N_{2h}$

## V. RESULTS AND DISCUSSION

In the following we present detailed numerical calculations of the differential cross section of a GaAs/AlGaAs parabolic quantum wire in presence of an uniform magnetic field as a function of  $\hbar\nu/E_g$ . The physical parameters used in our expressions are:  $E_g = 1.5177\text{eV}$ ,  $m_e = 0.0665m_0$ ,  $m_h = 0.45m_0$  (the heave-hole band). Taking the ratio 60:40 for the band-edge discontinuity [20, 21], the conduction and valence barrier heights are taken to be  $\Delta_e = 255\text{meV}$  and  $\Delta_h = 170\text{meV}$ . The oscillation frequencies  $\omega_{0e}$  and  $\omega_{0h}$  of the parabolic quantum wire are determined as

$$\omega_{0e(h)} = \frac{2}{d} \sqrt{\frac{2\Delta_{e(h)}}{m_{e(h)}}},$$

where  $d$  is the quantum wire diameter.

In Figs.1-3 we show the Raman spectra of the parabolic quantum wire in the  $X$  scattering configuration for different magnetic fields. The diameter  $d$  of the quantum wire is 2000 Å. The incident radiation frequency  $\hbar\nu_l = 1.68\text{ eV}$ . The positions of the singularities are defined by Eqs. (42),(43) and (44).

Figs. 3, 4 show the Raman spectra for the  $Z$  scattering configuration for the magnetic fields  $H = 8T$  and  $H = 16T$ . Other parameters coincide with those of Figs. 1-3. The structure of the differential cross section, as given in Figs. provides a transparent understanding of the energy subband structure of the parabolic quantum wire in a transverse magnetic field.

In the present work we have applied a simplified model for the electronic structure of the system. In a more realistic case we should consider the real band structure using a calculation model like that of the Luttinger-Kohn or Kane model. The above mentioned assumptions would lead to better results, but entail more complicated calculations. However, within the limits of our simple model we are able to take into account the essential physical properties of the discussed problem. The fundamental features of the differential cross section, as described in our work, should not change very much in real quantum wire case.

It can be easily proved that the singular peak in the differential cross section will be present irrespective of the model used for the subband structure and may be determined for the values of  $\hbar\nu_s$  equal to the energy difference between two subbands  $\hbar\nu_s = \hbar\nu_l - \hbar\nu = E_\alpha^e - E_\beta^e$ , where  $E_\alpha^e > E_\beta^e$  are electron energies in the subbands, respectively. At present there is a lack of experimental work on

this type of the ERS. Our major aim in performing these calculations is to stimulate experimental research in this

direction.

---

<sup>1</sup> Nagamune Y., Arakawa Y., Tsukamoto S, Nishioika M., Sasaki S. and Miura M. Photoluminescence spectra and anisotropic energy shift of GaAs quantum wires in high magnetic fields. *Phys. Rev. Lett.*, **69**, 2963 (1992).

<sup>2</sup> Plaut A.S., Lage H., Grambow P., Heitmann D., von Klitzing K. and Ploog K. Direct magneto-optical observation of a quantum confined one-dimensional electron gas. *Phys. Rev. Lett.*, **67**, 1642 (1991).

<sup>3</sup> Demel T., Heitmann D., Grambow P. and Ploog K. One-dimensional plasmons in AlGaAs/GaAs quantum wires. *Phys. Rev. Lett.*, **66**, 2657 (1991).

<sup>4</sup> Goni A.R., Pinczuk A., Weiner J.S., Dennis B.S., Pfeifer L. N. and West K. W. Observation of magnetoplasmons, rotons, and spin-flip excitations in GaAs quantum wires. *Phys. Rev. Lett.*, **70**, 1151 (1993).

<sup>5</sup> Choi K. K., Tsui D.C. and Palmateer S.C. Electron-electron interactions in GaAs-Al<sub>x</sub>Ga<sub>1-x</sub>As heterostructures. *Phys. Rev.*, **B 33**, 8216 (1986).

<sup>6</sup> Ford C.J.B., Thornton T.J., Newbery R., Pepper M., Ahmed H., Davies G. and Andrews D. Transport in GaAs heterojunction ring structures. *Superlatt. Microstruct.*, **4**, 451 (1988).

<sup>7</sup> Liu J., Ismail K., Lee K.Y., Hong J.M. and Washburn S. Cyclotron trapping, mode spectroscopy, and mass enhancement in small GaAs/Al<sub>x</sub>Ga<sub>1-x</sub>As rings. *Phys. Rev. B* **47**, 13039 (1993).

<sup>8</sup> Brum J. A., Bastard G., Chang L.L. and Esaki L. Energy levels in quasi uni-dimensional semiconductor heterostructures. *Superlatt. Microstruct.* **3**, 47 (1987).

<sup>9</sup> Bastard G., Brum J. A. and Ferreira R. Electronic states in semiconductor heterostructures. *Solid State Phys.*, **44**, 395 (1991).

<sup>10</sup> Lorenzoni A. and Andreani L.C. Rectangular quantum wires in a magnetic field: phase diagrams and subband dispersion. *Semicond. Sci. Technol.*, **14**, 1169 (1999).

<sup>11</sup> Cardona M. and Gntherodt G. Light Scattering in Solids V (Topics in Applied Physics 66) (Heidelberg: Springer, 1989).

<sup>12</sup> Cardona M. Lattice vibrations in semiconductor superlattices. *Superlatt. Microstruct.*, **7**, 183 (1990).

<sup>13</sup> Comas F., Trallero-Giner C. and Perez-Alvarez R. J. Interband-intraband electronic Raman scattering in semiconductors. *Phys. C: Solid State Phys.*, **19**, 6479 (1986).

<sup>14</sup> Pinczuk A. and Burstein E. Light Scattering in Solids I (Springer Topics in Applied Physics 8) ed. M. Cardona (Heidelberg: Springer, 1983).

<sup>15</sup> Wallis R.F and Mills D. L. Theory of Interband Raman Scattering in Semiconductors in Magnetic Fields. *Phys. Rev.*, **B 2**, 3312 (1970).

<sup>16</sup> Comas F., Trallero-Giner C., Lang I.G. and Pavlov S.T. Interband electron Raman scattering in semiconductors in crossed magnetic and electric fields. *Fiz. Tverd. Tela*, **27**, 57 (1985) (Engl. Transl. Sov. Phys. Solid State, **27**, 32 (1985)).

<sup>17</sup> Bechstedt F., Enderlein R. and Peuker K. Theory of inter-valence-band electronic Raman scattering in cubic semiconductors without and with an external electric field. *Phys. Status Solidi (b)* **68**, 43 (1975).

<sup>18</sup> Riera R., Comas F., Trallero-Giner C. and Pavlov S. T. Electron Raman scattering in semiconductor quantum wells. *Phys. Status Solidi (b)* **148**, 533 (1988).

<sup>19</sup> Betancourt-Riera R., Bergues J.M., Riera R., Marin J.L. One phonon assisted electron Raman scattering in spherical semiconductor quantum dots. *Physica*, **E 5**, 204 (2000).

<sup>20</sup> Burnett J.H., Cheong H.M., Westervelt R.M., Paul W., Hopkins P.F., Sundaram M., and Cossard A.C. Resonant inelastic light scattering in remotely doped wide parabolic GaAs/Al<sub>x</sub>Ga<sub>1-x</sub>As quantum wells. *Phys. Rev.*, **B 47**, 4524 (1993).

<sup>21</sup> Miller R.C., Kleinman D.A., and Gossard A.C. Energy-gap discontinuities and effective masses for GaAs-Al<sub>x</sub>Ga<sub>1-x</sub>As quantum wells. *Phys. Rev.*, **B 29**, 7085 (1984).

<sup>22</sup> Batey J., Wright S.L., and Di Maria D.J. Energy band-gap discontinuities in GaAs:(Al,Ga)As heterojunctions. *J. Appl. Phys.*, **57**, 484 (1985).